

Size-controlled preparation of peroxidase-like graphene-gold nanoparticle hybrids for the visible detection of norovirus-like particles

メタデータ	言語: eng 出版者: 公開日: 2018-08-27 キーワード (Ja): キーワード (En): 作成者: Ahmed, Syed Rahin, Takemeura, Kenshin, Li, Tian-Cheng, Kitamoto, Noritoshi, Tanaka, Tomoyuki, Suzuki, Tetsuro, Park, Enoch Y. メールアドレス: 所属:
URL	http://hdl.handle.net/10297/00025700

Size-controlled preparation of peroxidase-like graphene-gold nanoparticle hybrids for the visible detection of norovirus-like particles

Syed Rahin Ahmed,^a Kenshin Takemeura,^b Tian-Cheng Li,^c Noritoshi Kitamoto,^d Tomoyuki Tanaka,^e Tetsuro Suzuki,^f and Enoch Y. Park^{a,b*}

^a *Research Institute of Green Science and Technology, Shizuoka University, 836 Ohya, Suruga-ku, Shizuoka 422-8529, Japan*

^b *Graduate School of Integrated Science and Technology, Shizuoka University, 836 Ohya Suruga-ku, Shizuoka 422-8529, Japan*

^c *Department of Virology II, National Institute of Infectious Diseases, Gakuen 4-7-1, Musashi-Murayama, Tokyo 208-0011, Japan*

^d *School of Human Science and Environment, University of Hyogo, 1-1-12 Shinzaike-Honcho, Himeji, Hyogo 670-0092, Japan*

^e *Hidaka General Hospital, Gobo, Wakayama 644-0002, Japan*

^f *Department of Infectious Diseases, Hamamatsu University School of Medicine, 1-20-1 Higashi-ku, Handa-yama, Hamamatsu 431-3192, Japan*

*Corresponding to: Research Institute of Green Science and Technology, Shizuoka University, 836 Ohya, Suruga-ku, Shizuoka 422-8529, Japan.

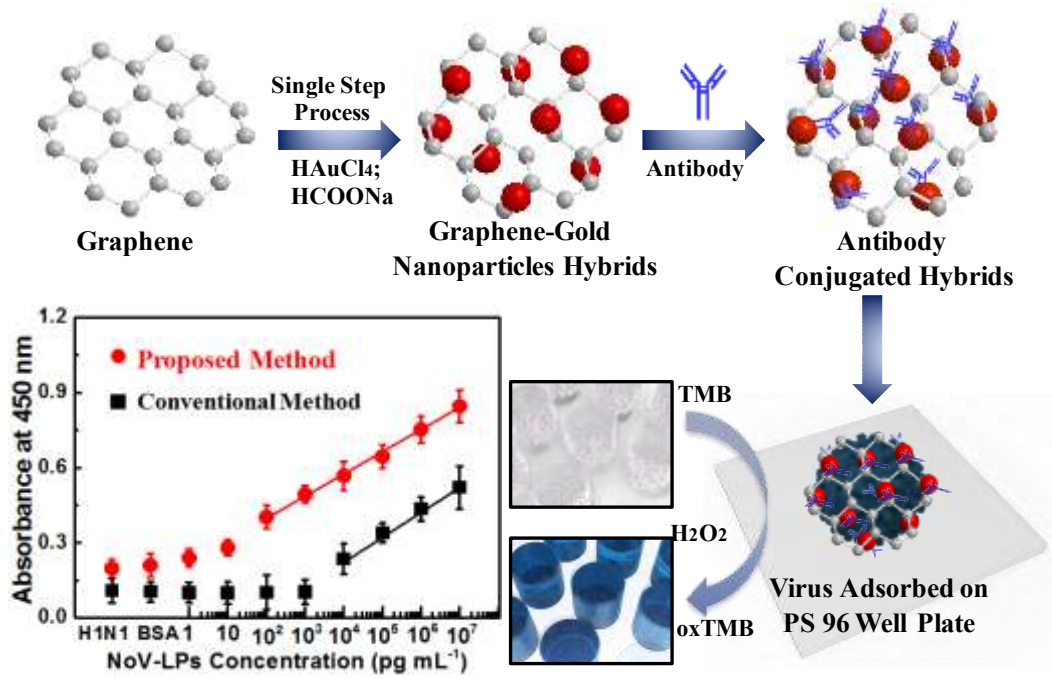
E-mail addresses: rahin_sust@yahoo.com (S.R. Ahmed), kenpi901@yahoo.co.jp (K. Takemura), litc@nih.go.jp (T.C. Li), kitamoto@shse.u-hyogo.ac.jp (N. Kitamoto), moqui-tom@maia.eonet.ne.jp (T. Tanaka), tesuzuki@hama-med.ac.jp (T. Suzuki), park.enoch@shizuoka.ac.jp (E.Y. Park)

ABSTRACT

A hybrid structure of graphene-gold nanoparticles (Grp-Au NPs) was designed as a new nanoprobe for colorimetric immunoassays. This hybrid structure was prepared using chloroauric acid, sodium formate and Grp flakes at room temperature. Au NPs attached strongly onto the Grp surface, and their size was controlled by varying the sodium formate concentration. The Raman intensity of the Grp-Au NP hybrids was significantly enhanced at $1,567\text{ cm}^{-1}$ and $2,730\text{ cm}^{-1}$ compared with those of pristine Grp because of the electronic interaction between Au NPs and Grp. The Grp-Au NPs with a hybrid structure catalyzed the oxidation of the peroxidase substrate 3,3,5,5-tetramethylbenzidine (TMB) with H_2O_2 , developing a blue color in aqueous solution. This catalytic activity was utilized to detect norovirus-like particles (NoV-LPs) in human serum. The enhanced colorimetric response was monitored using Ab-conjugated-Grp-Au NPs and found to depend on the NoV-LP concentration, exhibiting a linear response from 100 pg/mL to 10 $\mu\text{g/mL}$. The limit of detection (LOD) of this proposed method was 92.7 pg/mL, 112 times lower than that of a conventional enzyme-linked immunosorbent assay (ELISA). The sensitivity of this test was also 41 times greater than that of a commercial diagnostic kit. The selectivity of the Grp-Au NPs was tested with other viruses, and no color changes were observed. Therefore, the proposed system will facilitate the utilization of the intrinsic peroxidase-like activity of Grp-Au NPs in medical diagnostics. We believe that the engineered catalytic Grp-Au NP hybrids could find potential applications in the future development of biocatalysts and bioassays.

Keywords: Norovirus detection, Graphene, Gold nanoparticles, Nanohybrid structure, Peroxidase-like activity

Graphical Abstract



1. Introduction

Nanomaterial-based enzyme mimics have attracted research interest and have recently been shown to have potential applications in bioanalysis and environmental detection (Lin et al., 2014; Wei et al., 2103). Although natural enzymes, such as horseradish peroxidase (HRP), have been frequently used in recent decades, they have critical limitations for industrial applications, such as low stability under harsh conditions (temperature and pH) and relatively high costs of preparation, purification, and storage (Gao et al., 2007; Zhao et al., 2016). To overcome these limitations, the research interest in enzyme mimics has expanded from molecular to inorganic nanoscale materials, and as a result, highly organized artificial enzymes have been synthesized for a wide range of applications.

In particular, metal-based artificial enzymes, such as gold nanoparticles (Au NPs), magnetic NPs (Fe_3O_4 NPs) and platinum NPs (Pt NPs) have been discovered to possess intrinsic peroxidase-like activities (Ahmed et al., 2016; Gao et al., 2013; Liang et al., 2013; Sun et al., 2012; Zhao et al., 2015). In addition to single NPs, nanohybrids combining two or more NPs in single entity have also been intensively studied (Ahmed et al., 2016; Gao et al., 2014; Wang et al., 2014). Surprisingly, nanohybrids often exhibit synergistic effects that significantly enhance the catalytic performance and detection of analytes in the field of biosensors and immunoassays. To keep pace with developing sensitive detection of analytes, new generation of hybrid nanostructures with enhanced catalytic activity, high stability and low toxicity remains highly desirable to replace conventional peroxidase systems for practical applications.

Graphene (Grp)-based materials have been considered extremely versatile because of the extraordinary physicochemical properties that originate from Grp's unique

structure, including high mechanical strength, large surface area, good biocompatibility, high chemical stability and catalytic properties. Grp-based materials have shown promise for several advanced technological applications in the past few years (Li et al., 2008; Qu et al., 2011; Sing et al., 2011; Yang et al., 2013). Similarly, Au NPs have emerged as an interesting area of scientific research because of their favorable optical properties, biocompatibility, low toxicity, high intrinsic peroxidase-like activity and significant applications in photonics, catalysis, electronics and biomedicine (Daniel et al., 2004; Yeh et al., 2012). Based on these attractive properties, hybrid structures of Grp and Au NPs should enable the preparation of nanoprobe with great potential applications in colorimetric immunoassays. To date, several methods have been used to prepare hybrid structures of Grp-Au NPs, including thermal treatment, chemical reduction, and electrochemical or microwave-assisted methods. However, these methods have some limitations: they are time consuming, require high temperatures or involve complicated procedures.

Herein, a facile approach to prepare Grp-Au NP hybrids using sodium formate as a reducing and stabilizing agent of Au NPs on a Grp surface is presented. Because individual Grp and Au NPs have peroxidase-like activities, enhanced peroxidase-like performance was expected to be achieved via the rational combination of Au NPs and Grp. The attachment of Au NPs onto the Grp surface facilitated the conjugation of biomolecules, such as antibodies, onto the hybrid. Thus, a Grp-Au NP hybrid was further conjugated with an antiviral antibody (Ab) to obtain Ab-conjugated-Grp-Au NPs (Ab-Grp-Au NPs). These Ab-Grp-Au NPs were used as a robust nanoprobe for the quantitative, selective, and colorimetric detection of virus particles through the superior peroxidase-like activity of the hybrid (Scheme 1). In this study, norovirus-like particles (NoV-LPs)

was chosen as a model analyte because it is a leading cause of viral gastroenteritis outbreaks worldwide. NoVs are commonly transmitted through shellfish consumption and food and waterborne routes. However, the levels of enteric viruses in mussels are generally low (Morton et al., 2009; Schultz et al., 2007). Polymerase chain reaction (PCR)-based RNA detection has been widely used to identify causative agents. Simple and highly sensitive diagnostic systems for the detection of NoV antigens have not been established to date. To the best of our knowledge, this report is first to describe the sensitive colorimetric detection of NoV-LPs using inorganic nanohybrids as an artificial enzyme.

2. Experimental Section

2.1. Materials

Gold (III) chloride trihydrate ($\text{HAuCl}_4 \cdot 3\text{H}_2\text{O}$) and human serum (containing extremely complex biological matrices in dL, such as iron 35–180 μg , cholesterol 110–210 mg, triglyceride 30–175 mg, glucose 60–140 mg, endotoxin < 10 EU, and hemoglobin < 20 mg) were obtained from Sigma–Aldrich (St. Louis, MO, USA). Grp flakes (Model AO-3) were purchased from Graphene Supermarket (Calverton, NY, USA). Sodium formate (HCOONa), sodium acetate (NaOAc) and hydrogen peroxide (H_2O_2) were purchased from Wako Pure Chemical, Inc. (Osaka, Japan). *N*-(3-dimethylaminopropyl)-*N'*-ethylcarbodiimide (EDC) and *N*-hydroxysuccinimide (NHS) were purchased from Sigma-Aldrich (Milwaukee, WI, USA). The chromogenic substrate, 3,3',5,5'-tetramethylbenzidine (TMB) was obtained from Dojindo (Osaka, Japan). The

anti-influenza A virus hemagglutinin (HA) H1 Ab [B219M] (ab661189, Lot:GR40088–11) was obtained from Abcam, Inc. (Cambridge, UK). The influenza A (H3N2) HA monoclonal Ab (Anti-HA H3N2 MAb, Lot: HB04N0160) was acquired from Sino Biological, Inc. (Beijing, China). The anti-NoV Ab (NS-14), which is broadly reactive with the NoV genogroup II, was developed and characterized as previously described (Kitamoto et al., 2002; Kou et al., 2015). All experiments were conducted using high-purity deionized (DI) water ($> 18 \text{ M}\Omega\cdot\text{cm}$).

2.2. Preparation of Grp-Au NP hybrids

The one-step preparation of *in situ* hybrid nanostructures of Grp-Au NPs was conducted as follows: 1 mL of 20-mM $\text{HAuCl}_4\cdot 3\text{H}_2\text{O}$ and 2 mg of Grp flakes were mixed for 5 min under gentle stirring. Subsequently, 2 mL of 200–500-mM HCOONa was added, and the mixture was maintained at room temperature for 1 h. The Au cations attach to the Grp flakes via electrostatic interactions, are reduced by HCOONa to Au NPs, and are subsequently stabilized on the Grp surface.

2.3. Physicochemical properties of Grp-Au NP hybrids

Transmission electron microscopy (TEM) images were obtained using a TEM microscope (JEM-2100F, JEOL, Ltd., Tokyo, Japan) operated at 100 kV. The ultraviolet-visible (UV-vis) spectra of the nanostructured films were recorded using a Tecan Infinite M200 spectrophotometer (Infinite F500, TECAN, Ltd., Männedorf, Switzerland). Ab-conjugated Grp-Au NPs were monitored by Fourier transform infrared spectroscopy (FT-IR) (FT/IR 6300, JASCO Corp., Tokyo, Japan). The surface-enhanced Raman scattering (SERS) spectrum of the Grp-Au NP hybrids was recorded by Raman spectroscopy (NRS-

7100, JASCO Corporation, Tokyo, Japan). An X-ray powder diffractometer (RINT ULTIMA, Rigaku, Corp., Tokyo, Japan) was used to characterize the Grp-Au NP hybrids using Cu-K α radiation and a Ni filter. The data were collected over a range of $2\theta = 0\text{--}100^\circ$ at a scan rate of 0.01° per step and 10 s per point.

2.4. Construction of a recombinant baculovirus for the preparation of NoV-LPs

NoV cDNA (GII. 4 strain. Gen Bank accession no: LC153749) was isolated from human stool specimens in 2010. The full-length ORF2 of the cDNA was amplified by reverse transcriptase (RT)-PCR with the primers TCNF (5'-AGGATCCATGAAGATGGCGTCTCGAAT-3') and TCNR (5'-CTCTAGATTATAAAGCACGTCTACG-3') to produce fragments with *Bam*HI and *Xba*I sites, respectively, before and after the stop codon, respectively. The PCR product, which was digested with *Bam*HI and *Xba*I, was cloned into the corresponding site of a baculovirus transfer vector, pVL1393 (Pharmingen, San Diego, CA), yielding pVL1393-TCN-VP1. To produce the recombinant baculovirus, the transfer plasmid pVL1393-TCN-VP1 were mixed with CaculoGold (Pharmingen) and lipofectin (GIBCO-BRL, Gaithersburg, MD) and transfected into Sf9 cells (Riken Cell Bank, Tsukuba, Japan). The cells were incubated at 26.5°C in TC-100 medium (GIBCO-BRL) supplemented with 10% fetal bovine serum and 0.26% tryptose phosphate broth (Difco Laboratories, Sparks, MD, USA). The recombinant viruses were plaque-purified three times in Sf9 cells and designated as Ac[TCN-VP1].

2.5. Expression and purification of NoV-LPs

To achieve large-scale expression, an insect cell line from *Trichoplusia ni*, BTL-Tn

5B1-4 (Tn5) (Invitrogen, San Diego, CA, USA), was used. Tn5 cells that were infected with Ac[TCN-VP1] at a multiplicity of infection of 10 were cultured in EX-CELL™ 405 medium (JRH Biosciences, Lenexa, KS, USA) at 26.5°C, as described previously (Jiang et al., 1992). The supernatant that was obtained by centrifuging the infected culture at 10,000 × g for 60 min was further spun at 130,000 × g for 3 h in a Beckman SW32Ti rotor. The resulting pellet was resuspended and subjected to CsCl gradient centrifugation at 150,000 × g for 24 h at 10°C in a Beckman SW55Ti rotor. To estimate the abundance of NoV-LPs, the fractions were tested by Western blotting.

2.6. Conjugation of Grp-Au NP hybrids with anti-NoV Ab

One-milliliter volumes of Grp-Au NP hybrid solution (1 µg/mL), EDC (4 mM), and NHS (10 mM) were mixed and incubated for 10 min, and then, 1 µL of anti-NoV Ab (final concentration, 5 µg/mL) was added. The mixture was stirred at 4°C for 8 h. Finally, the supernatant and unbound antibodies were removed by centrifugation, and the Ab-conjugated Grp-Au NP (Ab-Grp-Au NP) hybrids were redispersed in 1 mL of high-purity DI water. In this process, antibodies bound the Grp-Au NP hybrids through an amide bond.

2.7. Colorimetric detection of NoV-LPs in complex biological matrices

To mimic the biological-sensing subjects of NoV-LPs in this experiment, a NoV-LP stock solution was serially diluted with human serum. The NoV-LP solution (100 µL) was then added to each well of a nonsterile polystyrene, 96-well, flat-bottom microtiter plate (Becton Dickinson Labware, NJ, USA) and incubated overnight at 4°C to allow the virus to adsorb onto the plates. Bovine serum albumin (BSA) (100 µL, 1 ng/mL) and influenza

virus A (H1N1) (100 μ L, 1 μ g/mL) were used as negative controls. The plates were then rinsed with phosphate-buffered saline (PBS; pH 7.5) and blocked with 100 μ L of 2% skim milk for 2 h at room temperature. One nanogram per milliliter of anti-NoV Ab-conjugated Grp-Au NPs (50 μ L) was added to the pre-adsorbed wells, and the plates were incubated for 1 h at room temperature. After washing three times with PBS (pH 7.5), 100 μ L of a mixture of TMB (5 mM) and H₂O₂ (10 mM) was added to each of the wells. The microplate was then incubated for 10 min at room temperature, which resulted in the development of a blue color depending on the concentration of NoV-LPs. Finally, 100 μ L of 10% H₂SO₄ was added to each well to stop the reaction. The absorbance at 450 nm was measured using a microplate reader (Model 680, Bio-Rad, Hercules, CA, USA). Based on the absorbance values at different NoV-LP concentration, a dose-dependent curve was constructed. The limit of detection (LOD) was calculated based on a previous report (Ahmed et al., 2016):

$$\text{LOD} \geq e \frac{3.3SD_{blank}}{b}$$

Where SD_{blank} and b indicate the standard deviation of the mean blank signal and the slope of the linear regression curve, respectively.

A commercially available diagnostic kit, NV-AD (III) (Denka Seiken Co., Ltd, Niigata, Japan), was also used to detect NoV-LPs according to the manufacturer's protocol. Serial dilutions of NoV-LPs were prepared and used in the assay. The diagnosis of NoV-LP detection was judged by the distinct colors that appeared in the 96-well plates at room temperature.

2.8. Conventional enzyme-linked immunosorbent assay (ELISA)

A conventional ELISA was performed to detect NoV-LPs as follows. NoV-LP (3 mg/mL) stock was diluted with PBS (pH 7.5) to a final titer of 10 μ g/mL. The NoV-LP solution (100 μ L) was then added to each well of a nonsterile polystyrene, 96-well, flat-bottom microtiter plate (Becton Dickinson Labware) and incubated overnight at 4°C to allow the virus to adsorb onto the plates. The plates were then rinsed with PBS (pH 7.5) and blocked with 100 μ L of 2% skim milk for 2 h at room temperature. The anti-NoV Ab (1 μ g/mL), the anti-H1N1 HA Ab (HA Ab66189; 1 μ g/mL) and 1-ng/mL BSA (100 μ L/well) were added to the pre-adsorbed wells, and the plates were incubated for 1 h at room temperature. The secondary antibody, HRP-labeled anti-mouse IgG (GE Healthcare UK Limited, UK), was then added to each well, followed by the chromogenic substrate TMB. The absorbance of the enzymatic product at 450 nm was measured using a microplate reader (Model 680, Bio-Rad) to quantify the interaction of the antibodies with the NoV-LPs.

3. Results and discussion

3.1. Preparation of Grp-Au NP hybrids and their application in virus detection

To avoid complicated multistep processes in Grp-Au NP hybrid preparation, a facile process was developed using HCOONa as a reducing agent for HAuCl₄, and the Au NPs spontaneously attached onto the Grp surface (Scheme 1). This simple, one-step protocol requires no additional stabilizing agents. The as-prepared Grp-Au NP hybrids facilitate the binding of antibodies because of the Au NPs attached to the Grp. Such nanohybrids could catalyze the oxidation of TMB by H₂O₂ to develop a blue color in aqueous solution;

this system was used here as a colorimetric sensor for NoV-LP detection in 96-well plates. In this system, the color change strongly depends on the nanohybrids concentration, which, in turn, depends on the NoV-LP concentration adhered onto the 96-well plates. This phenomenon was used to quantitatively detect NoV-LPs in this study.

[Scheme 1] A schematic illustration of one-step preparation of Grp-Au NP hybrids using Graphene flakes, HCOONa and HAuCl₄. The antibody was conjugated with Grp-Au NP hybrids through amide bonding, and the peroxidase-like activity was established based on the colorimetric detection of the virus deposited on 96-well plates. In the absence of Grp-Au NP hybrids, the TMB-H₂O₂ mixed solution was colorless. By contrast, in the presence of the Grp-Au NP hybrids, the oxidized TMB (oxTMB)-H₂O₂ solution produced a strong blue color.

3.2. Morphology of Grp-Au NP hybrids

The morphology of the Grp-Au NP hybrids is shown in Fig. 1A–D. Au NPs (shown as black dots in Fig. 1A) are strongly attached to the Grp surface and clearly distinguishable from pristine Grp (Fig. S1). The size of the Au NPs on the nanohybrids depended on the concentration of HCOONa used during the synthesis, i.e., ~10 nm sized Au NPs attached on Grp surface for 500-mM HCOONa (Fig. 1A), ~80 nm sized Au NPs attached on Grp surface for 400-mM HCOONa (Fig. 1B), ~200 nm sized Au NPs attached on Grp surface for 300-mM HCOONa (Fig. 1C), and ~500 nm sized Au NPs attached on Grp surface for 200-mM HCOONa (Fig. 1D).

The size and shape of the Au NPs became increasingly smaller and spherical as the concentration of HCOONa increased from 200-mM to 500-mM. In general, the lower

concentration of HCOONa (200-mM) was insufficient to reduce Au³⁺ to Au NPs and instead generated bigger sized and non-spherical Au NPs (500 nm, Fig. 1D) and at this stage, the particles shape is mostly controlled thermodynamically by surface free energies whose order is (111) < (100) < (110). Here, the low surface free energy facets such as {111} or {100} are dominantly exposed to form non-spherical shaped NPs. At high concentration, the reducing agent (HCOONa) is more strongly adsorbed on the (110) surface of Au NPs than on (100) and (111) respectively. The adsorbed HCOONa reduces the surface energy of 100 facet, thereby suppressing the anisotropic growth toward [111] direction and the morphology changes from non-spherical shape to the spherical shape with expanding the {100} facets (Kim et al. 2016).

[Figure 1] TEM images of Grp-Au NP hybrids: (A) Grp-Au NP hybrids synthesized with 500-mM HCOONa, (B) Grp-Au NP hybrids synthesized with 400-mM HCOONa, (C) Grp-Au NP hybrids synthesized with 300-mM HCOONa, and (D) Grp-Au NP hybrids synthesized with 200-mM HCOONa.

3.3. Spectroscopic investigation of Grp-Au NP hybrids

The UV spectroscopic study of Grp-Au NP hybrids revealed a broad absorbance spectrum with a characteristic plasmonic peak located at 550 nm, whereas no such peak was observed for pristine Grp (Fig. 2A). This broad peak was attributed to the coupling between the localized surface plasmon and Grp.

The structure of the Grp-Au NP hybrids was characterized using powder X-ray diffraction (XRD), and the results are shown in Fig. 2B. In the Grp flake samples (black line), the strong diffraction peak at $2\theta = 26.4^\circ$ and a small peak at $2\theta = 57.02^\circ$ were

identified as the (002) and (004) planes of graphite, respectively. However, several new diffraction peaks were observed (red line) in Grp-Au NP hybrids. The carbon peaks persisted at $2\theta = 26.4^\circ$ and 57.02° . The presence of crystalline Au in the Grp-Au NP hybrid was confirmed by the presence of the characteristic diffraction peaks of the face-centered cubic structure of bulk Au, i.e., (111), (200), (220), (311), (222) and (400) planes at 2θ values of 38.1 , 44.4 , 64.3 , 79.5 , 81.7 , and 97.9° , respectively. Grp-Au NP hybrids possess higher crystallinity than the Grp because of the presence of metal NPs in the hybrid structure, and they showed stronger diffraction patterns than the carbon face (Lee et al., 2014; Tai et al., 2010).

The SERS spectrum of Grp-Au NP hybrids was recorded using a laser Raman spectrometer (NRS-7100, Tokyo, Japan). The Raman spectrum contained a D band at $1,351\text{ cm}^{-1}$ because of the presence of local disorder, known as sp^3 defects, in the structure (Fig. 2C). A G-band analogous to that of sp^2 -containing graphitic carbon materials was observed at $1,567\text{ cm}^{-1}$ (Fig. 2C). Another band, present as a single strong peak, can be seen at $2,730\text{ cm}^{-1}$ in Fig. 2D, which corresponds to second-order scattering (2D mode) because of the participation of two phonons (Fig. 2D) (Yi et al., 2016). Clearly, the Raman intensity of the Grp-Au NP hybrids was enhanced by approximately three times at every point in compared with that of the pristine Grp because of the local optical field created by the electronic interaction between the Au NPs and Grp.

Compared with the pristine Grp, the Raman spectrum of the Grp-Au NP hybrids shows obvious peak shifts. On average, the D peak is red shifted by approximately 2 cm^{-1} , the G peak is red shifted by $\sim 5\text{ cm}^{-1}$, and the 2D peak is redshifted by $\sim 7\text{ cm}^{-1}$. The shift of the 2D peak is larger than those of the G and D peaks. Indeed, contact with Au NPs

significantly alters the electronic properties of Grp because of charge transfer from the Grp to GNPs. Moreover, the laser used in these experiments may excite the surface plasma of Au NPs, and electrons could be transferred from the Au NPs to Grp. Given these two reasons, charges will transfer between the Grp and Au NPs when the Au NPs are randomly distributed on the Grp surface. Ultimately, these charges are redistributed, and the locally charged Grp is then subjected to electrostatic attractive forces by the Au NPs. Additionally, electrostatic repulsion is caused by the adjacent charged Grp making contact with the Au NPs, stretching the adjacent charged Grp. These localized areas would be repulsed by each other and consequently give rise to strong tension in the Grp. Thus, both attractive and repulsive forces can induce strain in Grp, leading to a red shift in the Raman spectra of Grp (Zheng et al., 2015).

A significant difference in the zeta potential values between Grp (-13.9 mV) and the Grp-Au NP hybrids (-52.6 mV) was also observed. Clearly, all the above results indicate that the Au NPs were successfully synthesized and fixed on the Grp surface.

[Figure 2] Spectroscopic analysis of Grp-Au NP hybrids: (A) UV–visible spectra of Grp-Au NP hybrids, (B) XRD spectra of Grp-Au NP hybrids, and (C&D) SERS profile of Grp-Au NP hybrids.

3.4. Catalytic activity of Grp-Au NP hybrids

The catalytic effect of Au NPs size on hybrid structure was also assessed. To do that, 1 mg of four kinds of Grp-Au NP hybrids samples containing different sized Au NPs (10, 80, 200 & 500 nm) was mixed with TMB-H₂O₂ solution for 5 min separately and checked the absorbance of color developed (blue color). As shown in Fig. S2, the Grp-Au NP

hybrid solution (before H₂SO₄ was added to stop the reaction) showed stronger peroxidase-like activity upon the addition of the TMB-H₂O₂ solution than bare Grp. Moreover, smaller Au NPs (10-nm) exhibit higher peroxidase-like activities, presumably because of the large specific surface area (surface-to-volume ratio), which could facilitate interactions with large amounts of the colorimetric substrate. The optical density of the Grp-Au NP hybrids obtained with the 10-nm Au NP solution was approximately eight and six times higher than those of the Grp and the Grp-Au NP hybrids obtained using the 500-nm Au NP solution, respectively. Therefore, using smaller Au NPs (10-nm, spherical shape) to generate hybrid structures can accelerate the catalytic oxidation of TMB by H₂O₂. This finding can likely be applied to develop rapid and sensitive colorimetric biosensors for the detection of viral antigens.

3.5. Kinetic study of Grp-Au NP hybrids catalytic activity

To study the catalytic mechanism of nanohybrids, the apparent steady-state kinetic parameters were determined. A series of experiments was performed by varying substrate concentration while keeping constant the concentration of others. Based on a typical Michaelis-Menten kinetics (Fig. S3 A & B), Lineweaver-Burk double reciprocal plot was generated (Fig. S3 C & D). A comparison study of nanohybrids K_m and v_{max} values were also performed with HRP. As listed in Table S1, the K_m value of nanohybrids was higher than that of HRP toward H₂O₂, indicating that the nanohybrids had a lower affinity toward H₂O₂ than HRP. Also, the K_m value was lower than that of HRP toward TMB, indicating that the nanohybrids had a higher affinity toward TMB than HRP. The apparent catalytic constant (K^{app}_{cat}) of nanohybrids was calculated using equation $K^{app}_{cat} = (v_{max}/E_0)$, where E_0 denotes used nanohybrids concentration (mg mL⁻¹). The K^{app}_{cat} values for both TMB

and H₂O₂ were 7.0 mmol mg⁻¹ s⁻¹ and 4.4 × 10⁻¹ mmol mg⁻¹ s⁻¹, respectively. The nanohybrids possessed relatively high peroxidase-like activity which could provide a precondition to develop sensitive colorimetric immunoassay (Gao et al. 2013; Gao et al. 2014).

3.6. Preparation of NoV-LPs

The cell culture supernatants were collected from the Ac[TCN-VP1]-infected Tn5 cells 7 days post-infection. The NoV-LP proteins in the fractions of the CsCl gradient centrifugation were detected by Western blotting (Fig. 3A). Two major protein bands were observed at 58 and 55 kDa between fractions 10 and 14. The band at 58 kDa corresponded to the full-length NoV-LPs, and the band at 55 kDa was the partially processed NoV-LPs. The TEM images of NoV-LPs showed mono-dispersed spherical particles in fraction 11 (1.29 g/cm³) with a diameter of approximately 38 nm, similar to that of native NoV (Fig. 3B).

[Figure 3] Characterization of NoV-LPs: (A) Western blot analysis and (B) TEM images of NoV-LPs.

3.7. Optimal conditions for the colorimetric detection of NoV-LPs using Grp-Au NP hybrids

To obtain Grp-Au-NP hybrids with optimal catalytic activity, several parameters, such as pH, temperature, TMB concentration, H₂O₂ concentration and reaction time, were optimized. All of these parameters significantly affected the catalytic activity of Grp-Au-NP hybrids. The investigations were performed by varying the pH from 2 to 10, the

reaction time from 0 to 9 min, the H₂O₂ concentration from 0 to 20 mM, and the TMB concentration from 1 to 10 mM. The optimal pH and reaction time were approximately pH 7.5 and 5 min, respectively, and these parameters were adopted as the standard conditions for the subsequent measurements of the nanohybrids' catalytic activities (Fig. S4 A & B). The optimum conditions that maximized the peroxidase-like activities of the nanohybrids required a ratio of the H₂O₂ and TMB concentrations of 2:1 (Fig. S4 C & D). All the reactions were conducted at room temperature, which is a convenient temperature for sensing.

3.8. Colorimetric detection of NoV-LPs using Grp-Au NP hybrids

The specificity of anti-NoV Ab [NS14] against NoV-LPs was confirmed using a conventional ELISA. Fig. 4A shows that the optical density obtained for the anti-NoV Ab was higher than those of HA Ab 66189, anti-H3N2 HA MAb and BSA, implying the specificity of the anti-NoV Ab against NoV-LPs. Then, the conjugation of the anti-NoV Ab with the Grp-Au NP hybrids was confirmed using FTIR spectroscopy (Fig. 4B). The FTIR bands at 3,500–3,700 cm⁻¹ and 1,630–1,690 cm⁻¹ correspond to the amide N–H stretching and amide C=O stretching vibrational modes, respectively, which occur because of the chemical bonding between the Grp-Au NP hybrids and the anti-NoV Abs through an amide bond. However, no such peak was observed for bare Grp-Au NP hybrids.

The catalytic activity of the sensing system was investigated using four different reaction mixtures: a) anti-NoV Ab-conjugated Grp-Au NPs/TMB-H₂O₂; b) replacing the specific anti-NoV Ab with another Ab [anti H1N1 Ab] in reaction mixture a); c) removing

TMB from reaction mixture a); and d) removing H₂O₂ from reaction mixture a). In reaction mixture a), a deep blue color developed upon the addition of the TMB-H₂O₂ solution, and a strong characteristic absorption peak at 655 nm was also observed (Fig. 4C). However, none of the other mixtures (b, c, and d) showed this characteristic peak (Fig. 4C). These results suggest that the proposed sensing method is highly specific and shows color development only when the target virus, its specific Ab-conjugated Grp-Au NPs, TMB and H₂O₂ are present.

After the binding of the anti-NoV Ab to the Grp-Au NP hybrids and the selectivity of this novel sensing system were confirmed, a wide range of NoV-LPs concentrations were used to determine the linearity between the absorbance and the NoV-LP concentration. The sensitivity of this proposed system for NoV-LP detection was found to range from 100 pg/mL to 10 µg/mL. The LODs of our proposed method and the conventional ELISA method were calculated to be 92.7 pg/mL and 10.4 ng/mL, respectively (Fig. 4D). Thus, the proposed method was 112 times more sensitive than the conventional ELISA method. However, no significant color developed when using BSA or H1N1 virus (Fig. 4D).

[Figure 4] Specificity of anti-NoV Ab against NoV-LPs and the detection of NoV-LPs using Grp-Au NP hybrid nanostructures: (A) The specificity of the anti-NoV Ab against NoV LPs; (B) FTIR spectra of the antibody binding with Grp-Au NP hybrids; and (C) selectivity test of the proposed sensing method using the defined reaction mixture, (a) NoV-LPs with a specific Ab [NS14]-conjugated to Grp-Au NP hybrids and TMB-H₂O₂ and three separate modified mixtures as follows: b) substituting the specific Ab[NS14] with a non-specific Ab[anti-H1N1Ab66,189] in the defined reaction mixture; c) removing

TMB from the defined reaction mixture; and d) removing H₂O₂ from the defined reaction mixture. (D) The calibration curve of the absorbance versus the concentration of NoV-LPs. BSA was used as a negative control; H1N1 indicates the influenza virus A/New Caledonia/20/1999 (H1N1) that was used a control to test the system's specificity for NoV-LP detection. Closed circles (red) and closed squares (black) represent the proposed and conventional ELISA methods, respectively. Error bars in (A) and (D) indicate the standard deviation (n=3).

The sensitivity of the proposed method was compared with those of a commercially available NoV diagnostic kit (Table 1, Fig. S5). The visual color response to the detection of NoV-LPs in the commercial kit was as high as 1 ng/mL with a LOD of 3.8 ng/mL, indicating that our system is 41 times more sensitive than the commercial kit. We believe that this facile approach to prepare peroxidase-like hybrid nanostructures can be used to visibly detect infectious viruses with higher sensitivity. Moreover, this proposed method requires no sophisticated instrument and is, thus, applicable for low-cost, visible, point-of-care diagnosis

[Table 1] Comparison of NoV-LP detection using different methods

4. Conclusions

The *in situ* chemical deposition of Au NPs on a Grp surface was performed to prepare a new artificial enzyme. The Grp-Au NP hybrid exhibits unprecedented intrinsic peroxidase-like activity because of the high loading of Au NPs on the Grp nanocarrier. The superior peroxidase-like activity of Grp-Au NP hybrids was utilized to detect NoV-LPs. A significant color change was observed because of the oxidation of TMB in the

presence of the Grp-Au NP hybrid for NoV-LP detection. The sensitivity of this test was 112 and 41 times greater than those of conventional ELISA and commercial diagnostic kits, respectively. To the best of our knowledge, this value is the highest sensitivity for NoV detection achieved to date. Using this method, NoV can be detected over a wide range of concentrations. The proposed method of preparing the hybrids is a very simple, one-step process. In addition, the immunosensor showed a wide linear range and high specificity and sensitivity for NoV-LP detection, indicating that it has great potential for future real-life diagnostic applications.

Acknowledgment

This work was supported by the Suzuken Memorial Foundation of Japan.

Appendix. Supporting information

Supplementary data associated with this article can be found in the online version at

References

- Ahmed, S. R., Kim, J., Suzuki, T., Lee, J., Park, E. Y., 2016. *Biosens. Bioelectron.* 85, 503–508.
- Ahmed, S. R., Kim, J., Suzuki, T., Lee, J., Park, E. Y., 2016. *Biotechnol. Bioeng.* DOI: 10.1002/bit.25982.
- Daniel, M. C., Astruc, D., 2004. *Chem. Rev.* 104, 293–346.
- Gao, L., Zhuang, J., Nie, L., Zhang, J., Zhang, Y., Gu, N., Wang, T., Feng, J., Yang, D., Perrett, S., Yan, X., 2007. *Nat. Nano* 2, 577–583.
- Gao, Z., Hou, L., Xu, M., Tang, D., 2014. *Sci. Rep.* 4, 3966.
- Gao, Z., Xu, M., Hou, L., Chen, G., Tang, D., 2013. *Analytica Chimica Acta* 776, 79–86.
- Jiang, X., Wang, M., Graham, D. Y., Estes, M. K., 1992. *J. Virol.* 66, 6527–6532.
- Kim, H.S., Seo, Y.S., Kim, K., Han, J.W., Park, Y., Cho, S., 2016. *Nanoscale Res Lett.* 11, 230.
- Kitamoto, N., Tanaka, T., Natori, K., Takeda, N., Nakata, S., Jiang, X., Estes, M.K., 2002. *J. Clin. Microbiol.* 40, 2459–2465.

- Kou, B., Crawford, S.E., Ajami, N.J., Czako, R., Neill, F.H, Tanaka, T., Kitamoto, N., Palzkill, T.G., Estes, M.K., Atmar, R.L., 2015. *Clin. Vaccine Immunol.* 22,160–167.
- Lee, J., Kim, J., Ahmed, S. R., Zhou, H., Kim, J. M., Lee, J., 2014. *ACS Appl. Mater. Interfaces* 6, 21380–21388.
- Li, D., Kaner, R. B., 2008. *Science* 320, 1170–1171.
- Liang, M., Fan, K., Pan, Y., Jiang, H., Wang, F., Yang, D., Lu, D., Feng, J., Zhao, J., Lin, Y., Ren, J., Qu, X., 2014. *Acc. Chem. Res.* 47, 1097–1105.
- Morton, V., Jean, J., Farber, J., Mattison, K., 2009. *Appl. Environ. Microbiol.* 75, 4641–4643.
- Qu, F., Li, T., Yang, M., 2011. *Biosens. Bioelectron.* 26, 3927–3931.
- Schultz, A. C., Saadbye, P., Hoorfar, J., Nørrung, B., 2007. *Int. J. Food Microbiol.* 114, 352–356.
- Singh, V., Joung, D., Zhai, L., Das, S., Khondaker, S. I., Seal, S., 2011. *Prog. Mater. Sci.* 56, 1178–1271.
- Sun, H., You, J., Yang, M., Qu, F., 2012. *J. Power Sources* 205, 231–234.
- Tai, F. C., Wei, C., Chang, S. H., Chen, W. S., 2010. *J. Raman Spectrosc.* 41, 933–937.
- Wang, H., Li, S., Si, Y., Zhang, N., Sun, Z., Wu, H., Lin, Y., 2014. *Nanoscale* 6, 8107–

8116.

Wei, H., Wang, E., 2013. *Chem. Soc. Rev.* 42, 6060–6093.

Yang, L., Yan, X., 2013. *Anal. Chem.* 85, 308–312.

Yang, Y., Asiri, A. M., Tang, Z., Du, D., Lin, Y., 2013. *Mater. Today* 16, 365–373.

Yeh, Y. C., Creran, B., Rotello, V. M., 2012. *Nanoscale* 4, 1871–1880.

Yi, N., Zhang, C., Song, Q., Xiao, S., 2016. *Sci. Rep.* 6, 25134.

Zhao, Y., Zheng, Y., Kong, R., Lian Xia, L., Qu, F., 2016. *Biosens. Bioelectron.* 75, 383–388.

Zhao, Y., Zheng, Y., Zhao, C., You, J., Qu, F., 2015. *Biosens. Bioelectron.* 71, 200–206.

Zheng, X., Chen, W., Wang, G., Yu, Y., Qin, S., Fang, J., Wang, F., Zhang, X., 2015. *AIP Advances* 5, 057133.

Table 1.

Comparison of NoV-LP detection using different methods

Detection methods	NoV-LP concentration (pg/mL)					
	10 ²	10 ³	10 ⁴	10 ⁵	10 ⁶	10 ⁷
This study	+	+	+	+	+	+
Commercial kit	–	+	+	+	+	+
Conventional ELISA	–	–	–	+	+	+

*Note: + and –denote the positive and negative diagnoses, respectively.

Figure legends

Scheme. 1 A schematic illustration of the one-step preparation of Grp-Au NP hybrids using Graphene flakes, HCOONa and HAuCl₄. The antibody was conjugated with Grp-Au NP hybrids through amide bonding, and the peroxidase-like activity was established based on the colorimetric detection of the virus deposited on 96-well plates. In the absence of Grp-Au NP hybrids, the TMB-H₂O₂ mixed solution was colorless. By contrast, in the presence of the Grp-Au NP hybrids, the oxidized TMB (oxTMB)-H₂O₂ solution produced a strong blue color.

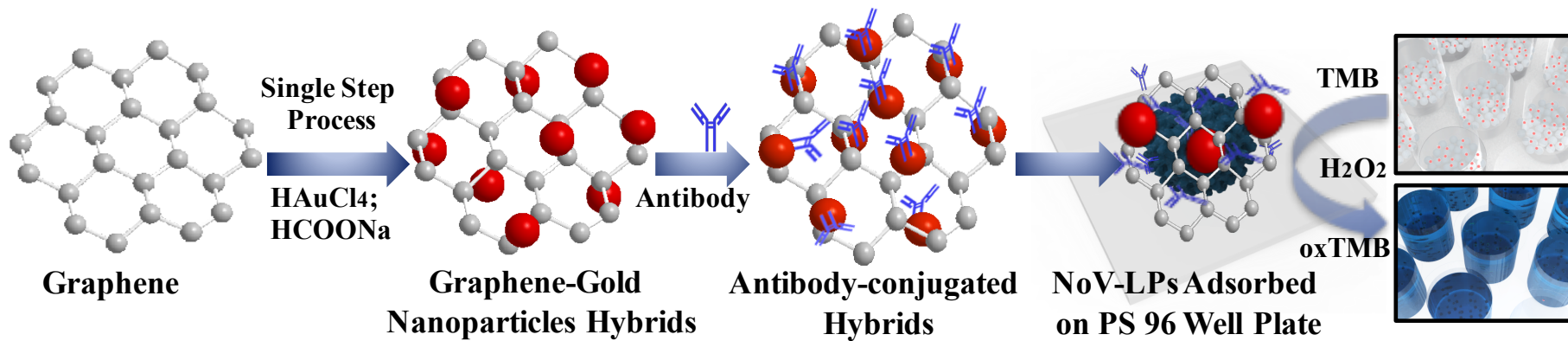
Fig. 1 TEM images of Grp-Au NP hybrids: (A) Grp-Au NP hybrids synthesized with 500-mM HCOONa, (B) Grp-Au NP hybrids synthesized with 400-mM HCOONa, (C) Grp-Au NP hybrids synthesized with 300-mM HCOONa, and (D) Grp-Au NP hybrids synthesized with 200-mM HCOONa.

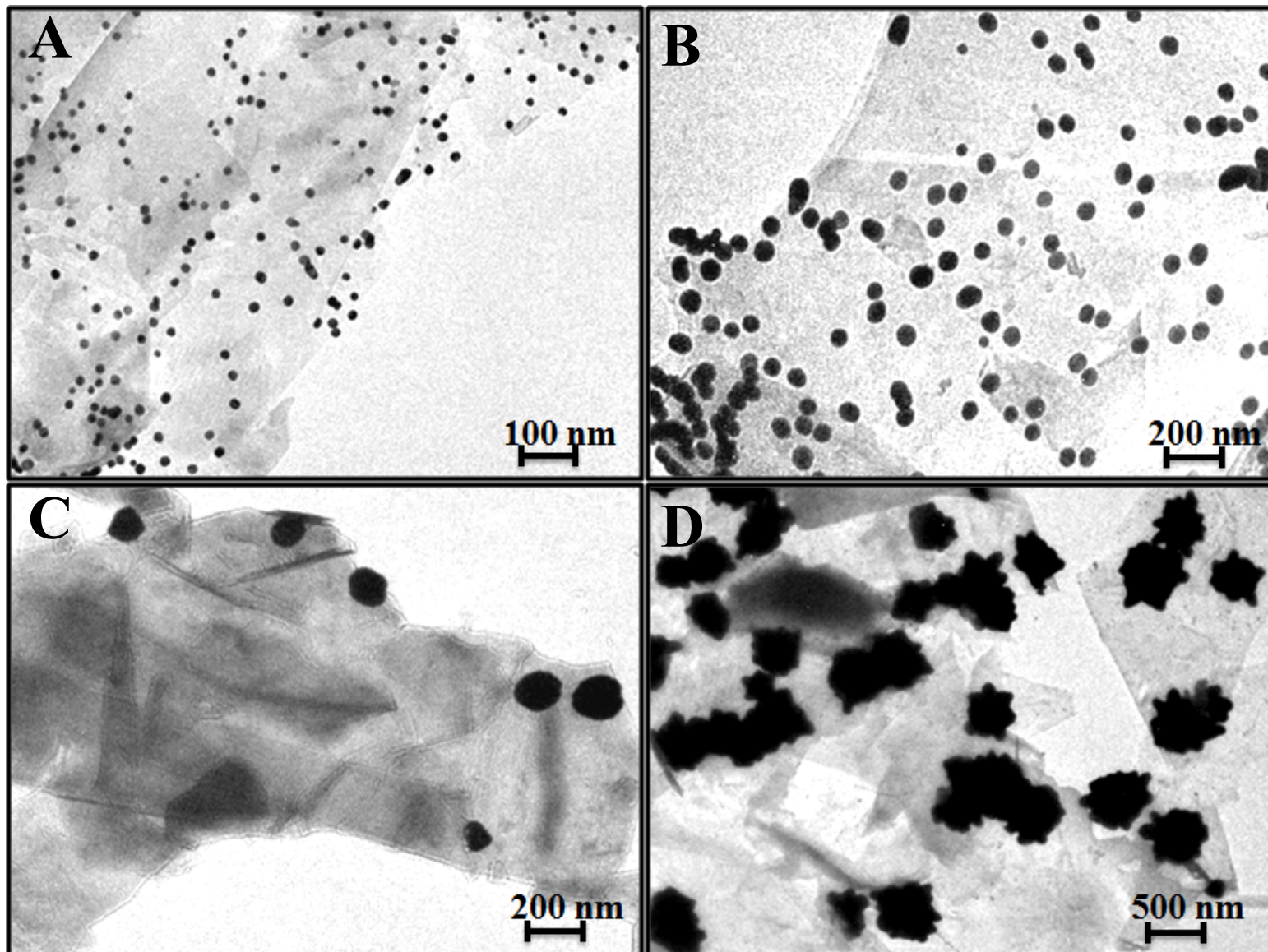
Fig. 2 Spectroscopic analysis of Grp-Au NP hybrids: (A) UV–visible spectra of Grp-Au NP hybrids, (B) XRD spectra of Grp-Au NP hybrids, and (C & D) SERS profile of Grp-Au NP hybrids.

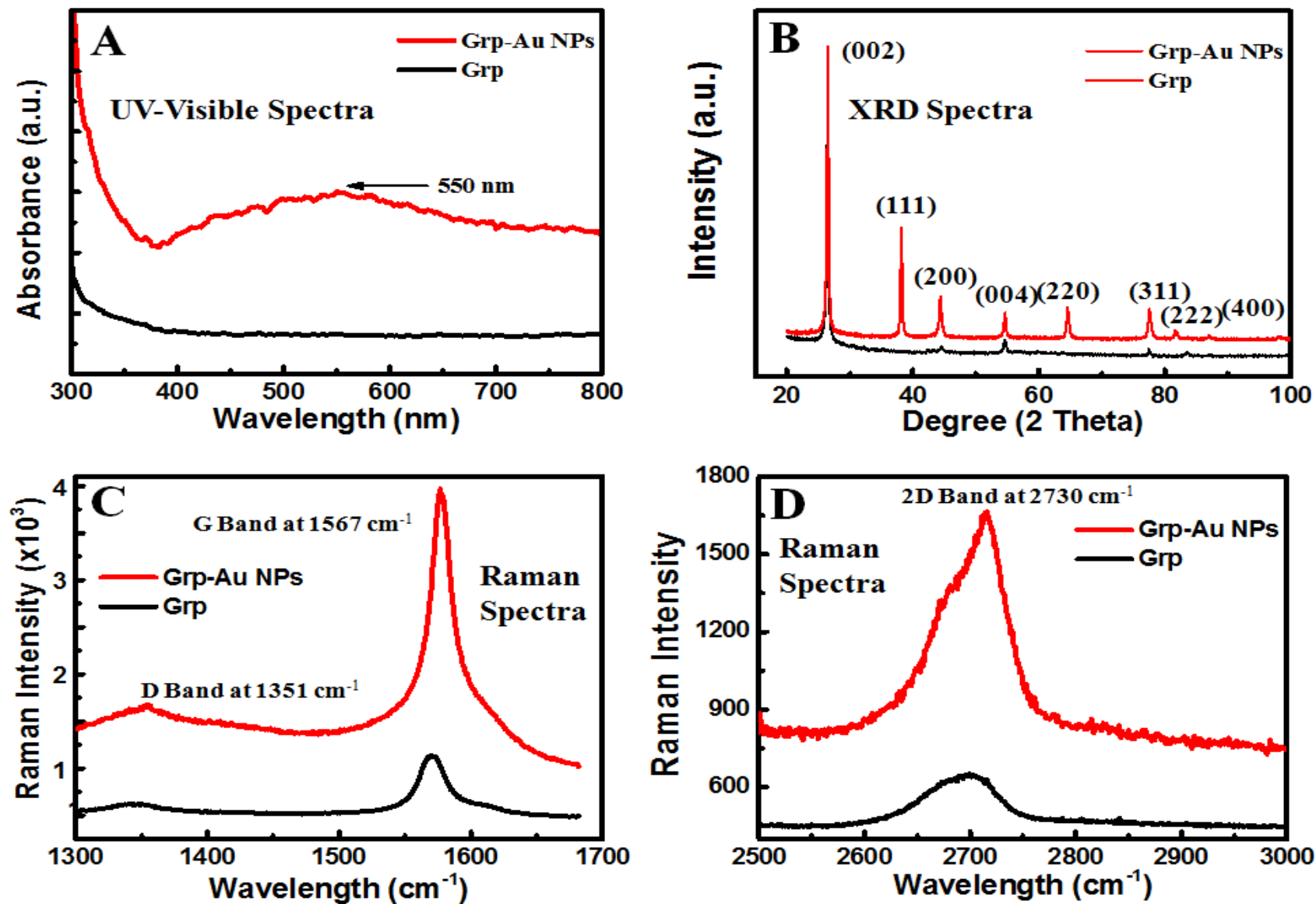
Fig. 3 Characterization of NoV-LPs: (A) Western blot analysis and (B) TEM images of NoV-LPs.

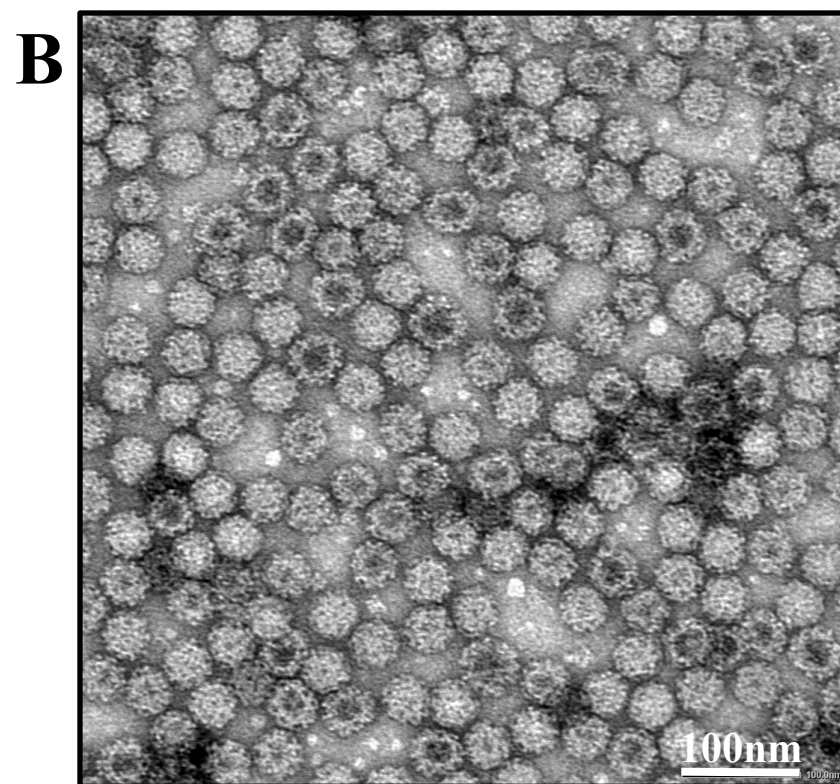
Fig. 4 Specificity of anti-NoV Ab against NoV-LPs and the detection of NoV-LPs using Grp-Au NP hybrid nanostructures: (A) The specificity of the anti-NoV Ab against NoV-LPs; (B) FTIR spectra of the Ab binding with Grp-Au NP hybrids; and (C) selectivity test of the proposed sensing method using the defined reaction mixture, (a) NoV-LPs with a

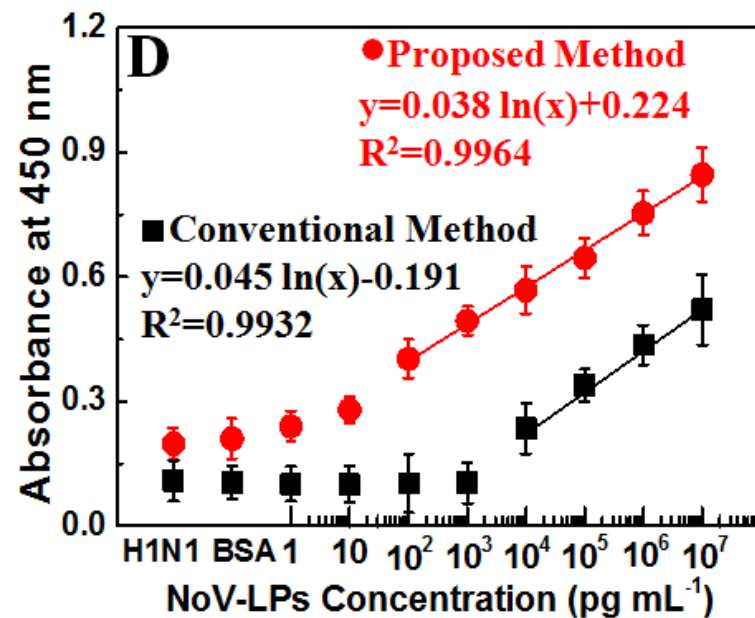
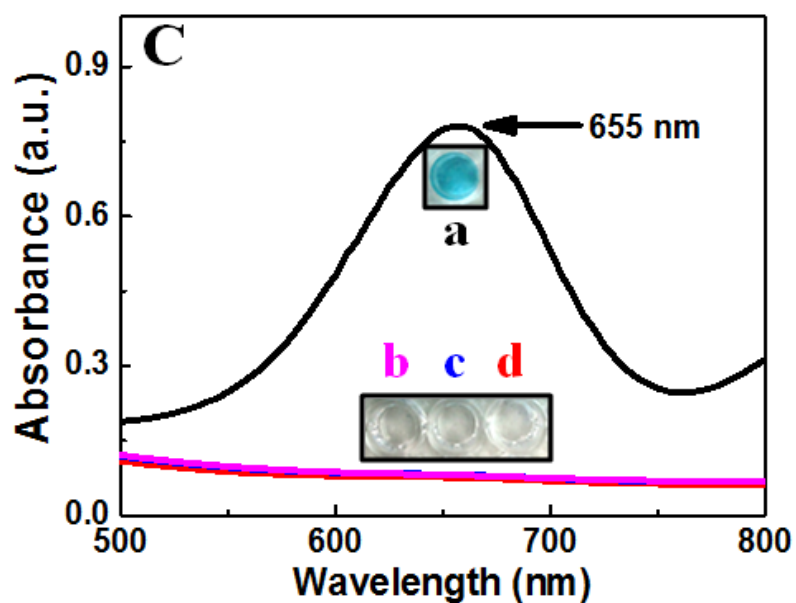
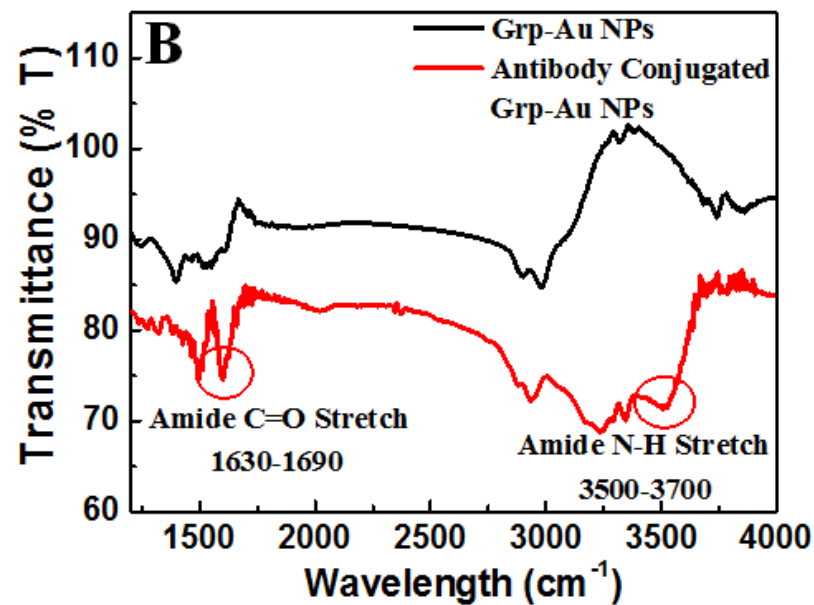
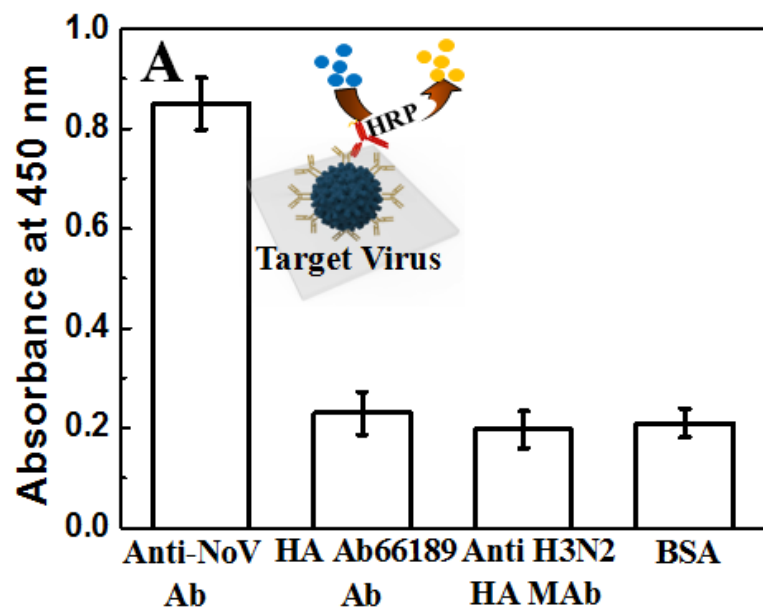
specific Ab [NS14]-conjugated to Grp-Au NP hybrids and TMB-H₂O₂ and three separate modified mixtures as follows: b) substituting the specific Ab [NS14] with a non-specific Ab [anti-H1N1Ab66,189] in the defined reaction mixture; c) removing TMB from the defined reaction mixture; and d) removing H₂O₂ from the defined reaction mixture. (D) The calibration curve of the absorbance versus the concentration of NoV-LPs. BSA was used as a negative control; H1N1 indicates the influenza virus A/New Caledonia/20/1999 (H1N1) that was used a control to test the system's specificity for NoV-LP detection. Closed circles (red) and closed squares (black) represent the proposed and conventional ELISA methods, respectively. Error bars in (A) and (D) indicate the standard deviation (n=3).











Supplementary information

Size-controlled preparation of peroxidase-like graphene-gold nanoparticle hybrids for the visible detection of norovirus-like particles

Syed Rahin Ahmed,^a Kenshin Takemeura,^b Tian-Cheng Li,^c Noritoshi Kitamoto,^d Tomoyuki Tanaka,^e Tetsuro Suzuki,^f and Enoch Y. Park^{a,b*}

^a *Research Institute of Green Science and Technology, Shizuoka University, 836 Ohya, Suruga-ku, Shizuoka 422-8529, Japan*

^b *Graduate School of Integrated Science and Technology, Shizuoka University, 836 Ohya Suruga-ku, Shizuoka 422-8529, Japan*

^c *Department of Virology II, National Institute of Infectious Diseases, Gakuen 4-7-1, Musashi-Murayama, Tokyo 208-0011, Japan*

^d *School of Human Science and Environment, University of Hyogo, 1-1-12 Shinzaike-Honcho, Himeji, Hyogo 670-0092, Japan*

^e *Hidaka General Hospital, Gobo, Wakayama 644-0002, Japan*

^f *Department of Infectious Diseases, Hamamatsu University School of Medicine, 1-20-1 Higashi-ku, Handa-yama, Hamamatsu 431-3192, Japan*

*Corresponding to: Research Institute of Green Science and Technology, Shizuoka University, 836 Ohya, Suruga-ku, Shizuoka 422-8529, Japan.

E-mail addresses: rahin_sust@yahoo.com (S.R. Ahmed), kenpi901@yahoo.co.jp (K. Takemura), litc@nih.go.jp (T.C. Li), kitamoto@shse.u-hyogo.ac.jp (N. Kitamoto), moqui-tom@maia.eonet.ne.jp (T. Tanaka), tesuzuki@hama-med.ac.jp (T. Suzuki), park.enoch@shizuoka.ac.jp (E.Y. Park)

Transmission electron microscopy (TEM) image of Graphene

Transmission electron microscopy (TEM) image of pristine graphene was obtained using a TEM (JEM-2100F, JEOL, Ltd., Tokyo, Japan) operated at 100 kV.

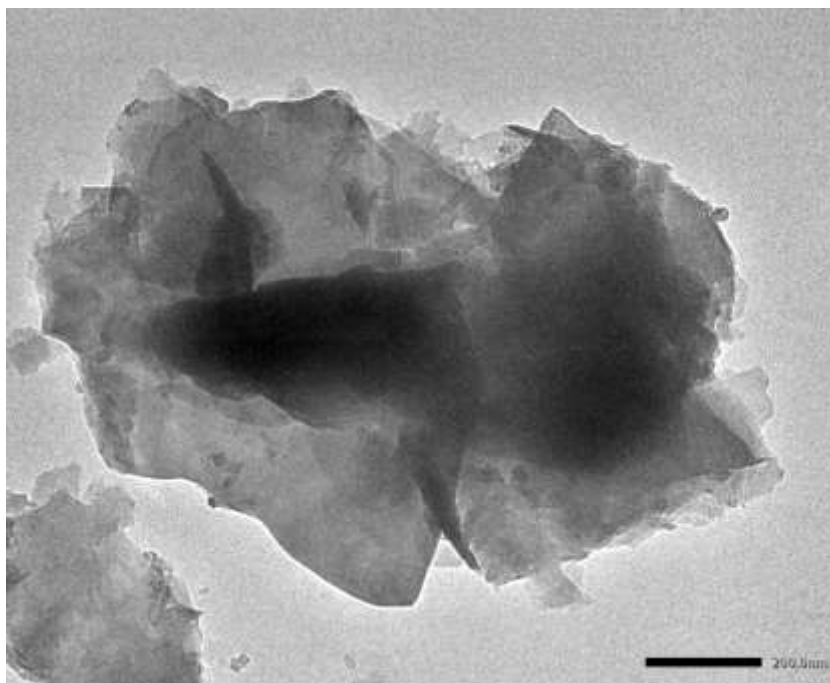


Fig. S1: TEM image of pristine graphene

Catalytic activity of Grp-Au NPs hybrids

A feasibility study of peroxidase-like activity was carried out using Grp-Au NPs hybrids and graphene. Different sized Au NPs attached on graphene surface were studied to check Au NPs size depended catalytic activities here. As shown in Fig. S2, the Grp-Au NPs hybrids solution (before adding H_2SO_4 to stop the reaction) showed stronger peroxidase-like activity upon addition of TMB- H_2O_2 solution in compare to bare graphene. Moreover, Au NPs with smaller size showed higher peroxidase-like activity due to large surface to volume ratio which could facilitate to interact with huge amounts of colorimetric substrate. The optical density of the Grp-Au NPs hybrids with 10 nm Au NPs solution was about eight and six times higher than that of the graphene and Grp-Au NPs hybrids with 500 nm Au NPs solution, respectively, which indicates that adding of smaller sized Au NPs to a hybrid structure can accelerate the catalytic oxidation of TMB with H_2O_2 . This finding could be applied to develop rapid and sensitive colorimetric biosensors for infectious viral detection.

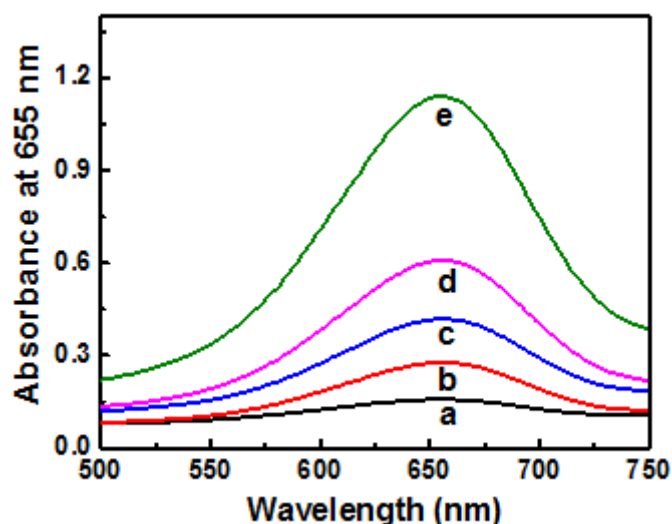


Fig. S2: A comparison study of catalytic activity: (a) pristine graphene; (b) Grp-Au NPs hybrids synthesized with 200 mM HCOONa (500 nm Au NPs size); (c) Grp-Au NPs

hybrids synthesized with 300 mM HCOONa (200 nm Au NPs size); (d) Grp-Au NPs hybrids synthesized with 400 mM HCOONa (80 nm Au NPs size); (e) Grp-Au NPs hybrids synthesized with 500 mM HCOONa (10 nm Au NPs size).

Kinetic study of Grp-Au NP hybrids catalytic activity

To study the catalytic mechanism of nanohybrids, the apparent steady-state kinetic parameters were determined by changing the concentration of TMB and H₂O₂ in this system, respectively. Here, the kinetic analysis was carried out by using 20 μ L Grp-Au NP hybrids (1 mg mL⁻¹) in a reaction volume of 100 μ L PBS buffer solution (pH = 7.5) with 5 mM TMB or 10 mM H₂O₂. A series of experiments were performed by varying substrate concentration while keeping constant the concentration of others. At a certain range, typical Michaelis-Menten curves were obtained for nanohybrids with both substrates (Fig. S3 A & B). To further analysis of basic parameters, Lineweaver-Burk double reciprocal plot was used. The reciprocal of initial rate was proportional to the reciprocal of substrate (TMB and H₂O₂) concentration, which was fitted to the double reciprocal of the Michaelis-Menten equation, $\frac{1}{v} = \frac{K_m}{v_{max}} \cdot \frac{1}{[S]} + \frac{1}{v_{max}}$ (Fig. S3 C& D), where v , K_m , v_{max} and $[S]$ denote the initial rate, the Michaelis–Menten constant, the maximum reaction rate and the substrate concentration, respectively. A comparison study of nanohybrids K_m and v_{max} values were also performed with HRP (Table S1). The apparent catalytic constant (K^{app}_{cat}) of nanohybrids was calculated using equation $K^{app}_{cat} = (v_{max}/E_0)$, where E_0 denotes used nanohybrids concentration (mg mL⁻¹). The K^{app}_{cat} values for both TMB and H₂O₂ were 7.0 mmol mg⁻¹ s⁻¹ and 4.4×10^{-1} mmol mg⁻¹ s⁻¹, respectively.

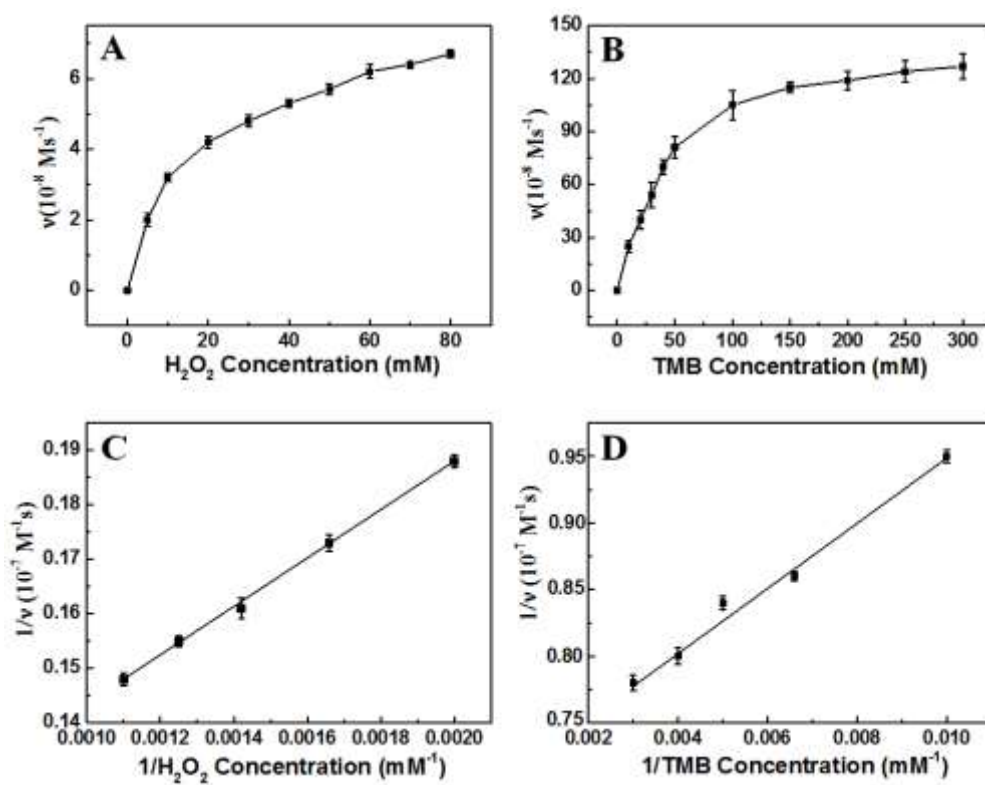


Fig. S3: Steady-state kinetic assay and catalytic characteristics of Grp-Au NPs hybrids toward various components: (A, C) 5 mM TMB and different-concentration H_2O_2 , (B, D) 10 mM H_2O_2 and different-concentration TMB.

Optimal conditions for the colorimetric detection of NoV-LPs using Grp-Au NP hybrids

To obtain Grp-Au-NP hybrids with optimal catalytic activity, several parameters, such as pH, temperature, TMB concentration, H₂O₂ concentration and reaction time, were optimized. All of these parameters significantly affected the catalytic activity of Grp-AuNP hybrids. The investigations were performed by varying the pH from 2 to 10, the reaction time from 0 to 9 min, the H₂O₂ concentration from 0 to 20 mM, and the TMB concentration from 1 to 10 mM. The optimal pH and reaction time were approximately pH 7.5 and 5 min, respectively, and these parameters were adopted as the standard conditions for the subsequent measurements of the nanohybrids' catalytic activities (Fig.S4A and B). The optimum conditions that maximized the peroxidase-like activities of the nanohybrids required a ratio of the H₂O₂ and TMB concentrations of 2:1 (Fig. S4 C and D). All the reactions were conducted at room temperature, which is a convenient temperature for sensing.

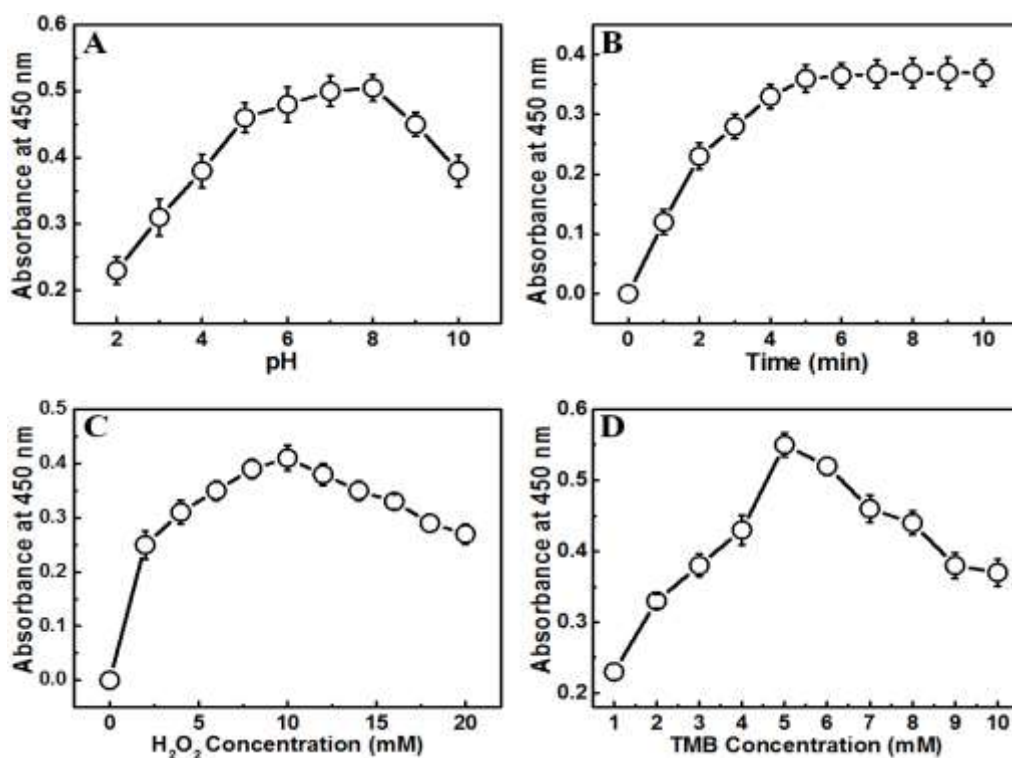


Fig. S4: The peroxidase-like activity of Grp-Au NP hybrids(1µg/mL) at different (A) pH values (Reaction conditions: 5-mM TMB and 10-mM H₂O₂); (B) Reaction times

(Reaction conditions: 5-mM TMB, 10-mM H₂O₂ and pH 7.5 at 25°C); (C) Varied H₂O₂ concentrations with a fixed TMB concentration of 5 mM; and (D) Varied TMB concentrations with a fixed H₂O₂ concentration of 10 mM. The reaction conditions were fixed at pH 7.5 and 25°C. The error bars denote the standard deviation (n=3).

Detection of NoV-LPs by commercial diagnostic kit

In this study, a direct and complementary comparison of the detection ability with commercially available diagnostic kit (NV-AD (III), Denka seiken CO., LTD, Niigata, Japan) was also investigated. Different NoV-LPs titers were prepared and performed according to manufacturer's protocol. Positive and negative NoV-LPs diagnostic results were obtained from different significant color appeared on 96 well plates at room temperature and shown in Fig. S5.

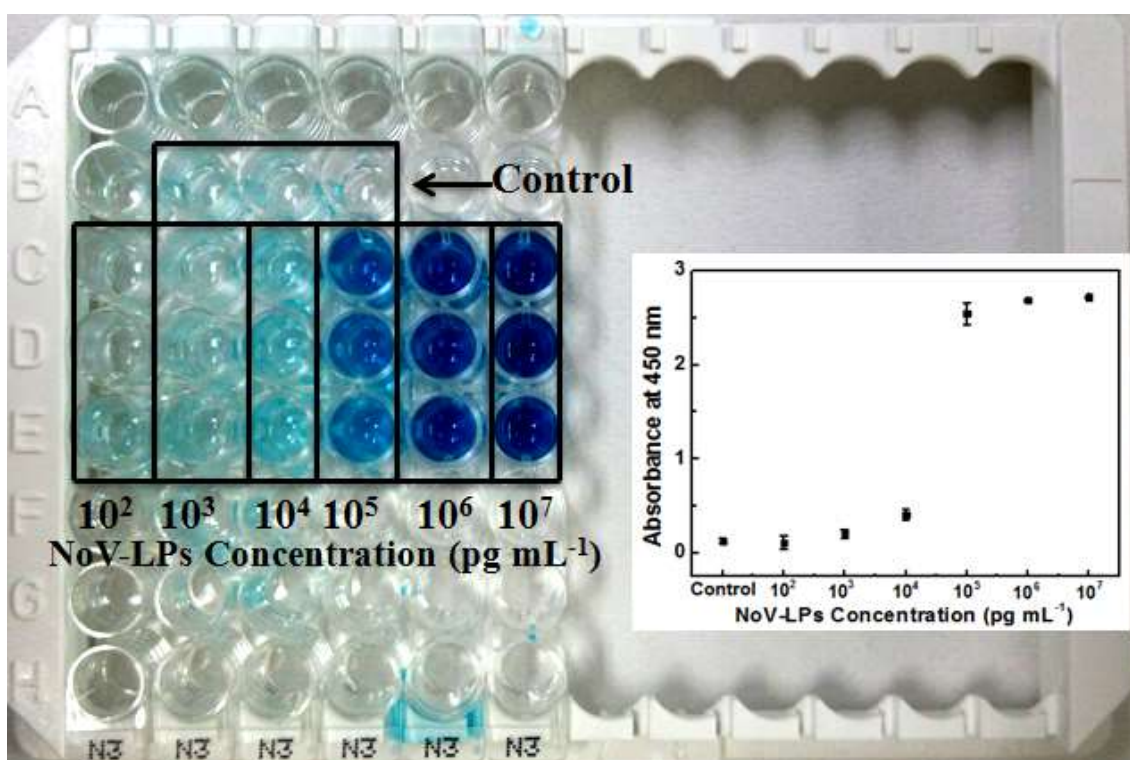


Fig. S5: Visual detection of NoV-LPs using commercial kit (inset: absorbance spectra Vs NoV-LPs curve).

Table S1: A comparison study of kinetic parameters between nanohybrids and HRP

Enzyme mimics	K_m (mM)		v_{\max} (10^{-5} mM \cdot s $^{-1}$)	
	TMB	H ₂ O ₂	TMB	H ₂ O ₂
Grp-Au NPs	0.03	27.26	140	8.93
HRP (Gao et al. 2014)	0.43	3.70	10	8.71